# A Dual-Function MOF for High Proton Conduction and Sensitive Detection of Ascorbic Acid

*Shu-Fang Zhou,*[a] *Biao-Biao Hao,*[a] *Tian Lin,*[a] *Chen-Xi Zhang*[*ab] *and Qing-Lun Wang*[*cd]

a College of Chemical Engineering and Materials Science, Tianjin University of Science and Technology, Tianjin 300457, P. R. China

b Key Laboratory of Brine Chemical Engineering and Resource Eco-utilization, Tianjin University of Science and Technology, Tianjin 300457, P. R. China

c Key Laboratory of Advanced Energy Materials Chemistry (Ministry of Education), Nan kai University, Tianjin 300071, P. R. China

d College of Chemistry, Nan kai University, Tianjin 300071, P. R. China

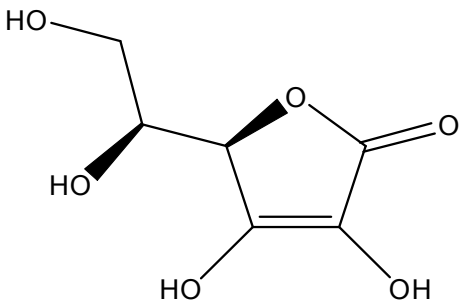


**Scheme S1.** Molecular structure of Ascorbic Acid (AA)

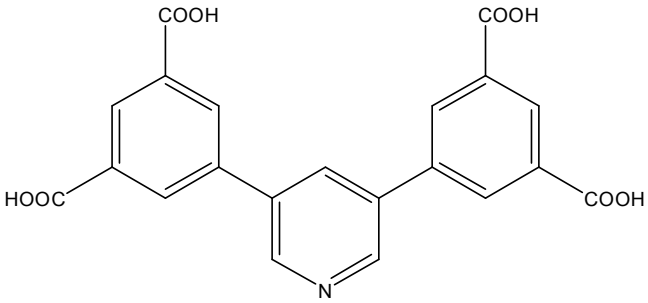


**Scheme S2.** Molecular structure of $H_4$BDPP

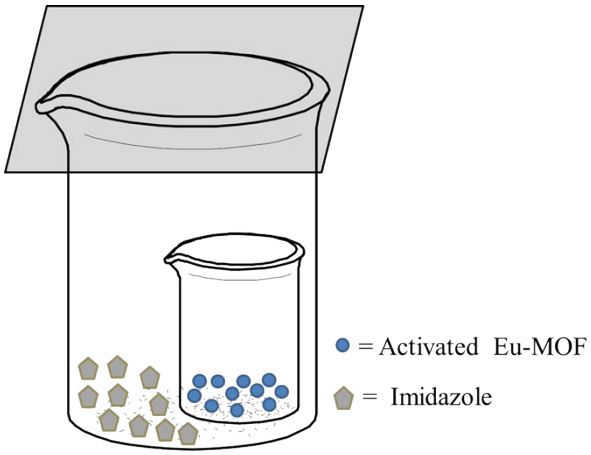


**Scheme S3.** Schematic for encapsulating imidazole molecules into Eu-MOF via vaporization method.

**Table S1.** Crystal data and structure refinement for Eu-MOF

| complex | Eu-MOF |
|---|---|
| Formula | $C_{47}H_{41}Eu_2N_4O_{23}$ |
| *Mr* | 1333.76 |
| T/K | 155(40) |
| Crystal system | monoclinic |
| Space group | $P2_1/c$ |
| *a*/ Å | 15.1205(6) |
| *b* / Å | 10.7089(7) |
| *c*/ Å | 15.3715(10) |
| $\alpha$ /° | 90 |
| $\beta$ /° | 95.057 |
| $\gamma$/° | 90 |
| Z | 2 |
| Volume /Å$^3$ | 2479.3(2) |
| $\rho$ /g cm$^{-3}$ | 1.787 |
| $\mu$ /mm$^{-1}$ | 2.597 |
| *F*(000) | 1322.0 |
| Crystal size /mm$^3$ | 0.20×0.18×0.12 |
| $2\theta$ /° | 6.178 to 50.018 |
| Reflections/ unique | 15750/4361 |
| $R_{(int)}$ | 0.1084 |
| Data / restraints / parameters | 4361/84/357 |
| GOF on $F^2$ | 1.098 |
| $R_1$ [I>2δ(I)] | 0.0648 |
| w$R_2$ [I>2δ(I)] | 0.1539 |
| $R_1$ (all data) | 0.0904 |
| w$R_2$ (all data) | 0.1848 |

**Table S2.** Selected Bond Lengths (Å) and angles (°) of Eu-MOF

| Eu-MOF | | | |
|---|---|---|---|
| Eu(4)- Eu(4)#1 | 4.0437(8) | Eu(4)-O(1)#2 | 2.641(6) |
| Eu(4)-O(9) | 2.459(6) | Eu(4)-O(1)#3 | 2.366(6) |
| Eu(4)-O(22) | 2.368(6) | Eu(4)-O(2)#2 | 2.454(7) |
| Eu(4)-O(24) | 2.518(6) | O(1)-Eu(4)#6 | 2.641(6) |
| Eu(4)-O(29) | 2.451(6) | O(1)-Eu(4)#7 | 2.366(6) |
| Eu(4)-O(44) | 2.450(7) | O(2)-Eu(4)#6 | 2.454(7) |
| Eu(4)-O(51) | 2.457(7) | | |
| | | | |
| O(9)-Eu(4)-Eu(4)#1 | 66.23(14) | O(44)-Eu(4)-O(51) | 71.7(3) |
| O(22)-Eu(4)-Eu(4)#1 | 68.41(15) | O(51)-Eu(4)-Eu(4)#1 | 114.47(18) |
| O(9)-Eu(4)-O(24) | 68.89(19) | O(44)-Eu(4)-O(2)#2 | 76.9(2) |
| O(22)-Eu(4)-O(9) | 133.2(2) | O(51)-Eu(4)-O(9) | 138.6(3) |

| | | | |
|---|---|---|---|
| O(9)-Eu(4)-O(1)#2 | 71.8(2) | O(44)-Eu(4)-O(1)#2 | 114.5(2) |
| O(22)-Eu(4)-O(24) | 143.2(2) | O(51)-Eu(4)-O(24) | 72.7(2) |
| O(22)-Eu(4)-O(29) | 146.0(2) | O(51)-Eu(4)-O(1)#2 | 136.3(2) |
| O(22)-Eu(4)-O(44) | 78.9(2) | O(1)#2-Eu(4)-Eu(4)#1 | 33.90(14) |
| O(22)-Eu(4)-O(51) | 72.3(2) | O(1)#3-Eu(4)-Eu(4)#1 | 38.51(14) |
| O(22)-Eu(4)-O2#2 | 91.2(2) | O(1)#3-Eu(4)-O(22) | 78.6(2) |
| O(29)-Eu(4)- O(9) | 74.5(2) | O(1)#3-Eu(4)-O(51) | 84.3(2) |
| O(29)-Eu(4)-O(51) | 99.8(2) | O(1)#3-Eu(4)-O(2)#2 | 121.5(2) |
| O(44)-Eu(4)- O(9) | 135.6(2) | O(2)#2-Eu(4)-O(51) | 146.7(3) |
| O(29)-Eu(4)-O(1)#2 | 123.0(2) | O(2)#2-Eu(4)-Eu(4)#1 | 84.05(13) |
| O(29)-Eu(4)-O(2)#2 | 77.5(2) | O(2)#2-Eu(4)-O(9) | 73.3(2) |
| O(22)-Eu(4)-O(1)#2 | 67.3(2) | O(1)#3-Eu(4)-O(9) | 73.3(2) |
| O(24)-Eu(4)-O(1)#2 | 139.3(2) | O(1)#3-Eu(4)-O(29) | 134.5(2) |
| O(44)-Eu(4)- O(24) | 100.7(2) | O(2)#2-Eu(4)-O(1)#2 | 51.16(19) |
| O(44)-Eu(4)- O(29) | 67.4(2) | Eu(4)#7-O1-Eu(4)#6 | 107.6(2) |
| O(29) -Eu(4)- O(24) | 52.7(2) | O(1)#3-Eu(4)-O(1)#2 | 72.4(2) |
| O(22)-Eu(4)-Eu(4)#1 | 117.58(16) | O(1)#3-Eu(4)-O(24) | 86.8(2) |
| O(29)-Eu(4)-Eu(4)#1 | 139.94(16) | O(1)#3-Eu(4)-O(44) | 151.1(2) |
| O(44)-Eu(4)-Eu(4)#1 | 141.56(15) | O(2)#2-Eu(4)-O(24) | 124.8(2) |

Symmetry Codes: #1 = -X, 2-Y,1-Z; #2 = -X, 1/2+Y, 1/2-Z; #3 = +X,3/2-Y,1/2+Z; #4 = 1-X, -1/2+Y, 1/2-Z; #5 = 1-X, 1/2+Y, 1/2-Z; #6 = -X, -1/2+Y, 1/2-Z; #7 = +X, 3/2-Y, -1/2+Z

**Table S3.** Comparison of the proton conductivity values of Im@Eu-MOF with other proton conducting materials containing guest molecules.

| Materials | Conductivity ($S \cdot cm^{-1}$) | Conditions | References |
|---|---|---|---|
| Im@Eu-MOF | $4.53\times10^{-4}$ | 348 K, 98% RH | This work |
| Im-Cu@(NENU-3a) | $3.16\times10^{-4}$ | 70℃, 90% RH | 40 |
| Im@Td-PPI | $9.04\times10^{-5}$ | 90℃ | 39 |
| Im@Td-PNDI | $3.49\times10^{-4}$ | 90℃ | 39 |
| polyPtC-Im | $1.5\times10^{-5}$ | 120℃ | 21 |
| $[Zn(HPO_4)(H_2PO_4)_2](ImH_2)_2$ | $2.6\times10^{-4}$ | 130℃ | 41 |
| Im@[Al($\mu_2$-OH)(1,4-ndc)] | $2.2\times10^{-5}$ | 120℃ | 34 |
| Im@[Al($\mu_2$-OH)(1,4-bdc)] | $1.0\times10^{-7}$ | 120℃ | 34 |
| OF⊂ Im | $2.4\times10^{-5}$ | 120℃ | 42 |

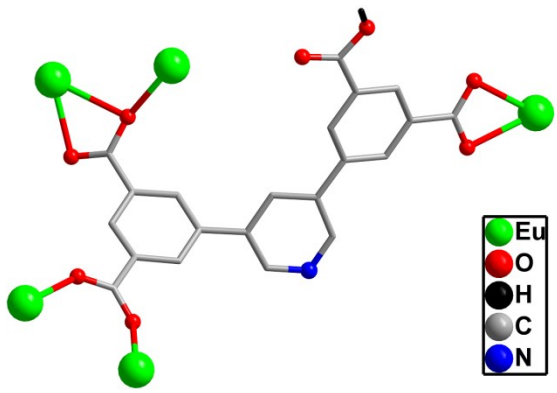


**Figure S1.** Coordination mode of the ligand in Eu-MOF

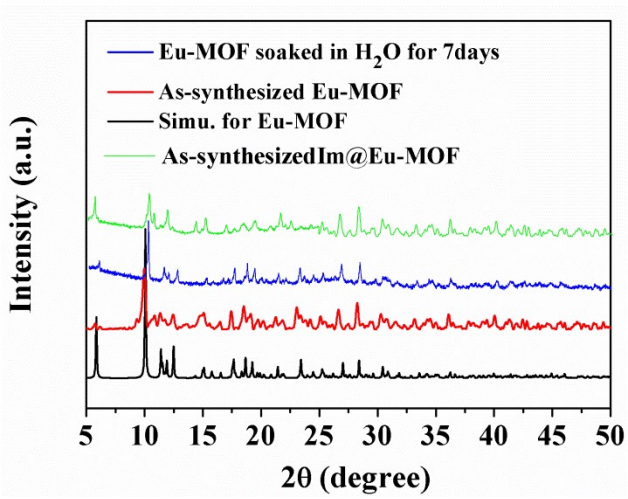


**Figure S2.** PXRD spectra of Eu-MOF in different states and experimental PXRD profiles of Im@Eu-MOF

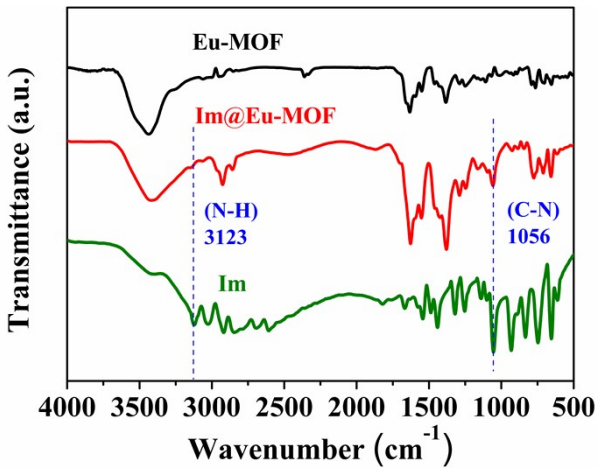


**Figure S3.** FT-IR spectra of Eu-MOF, Im@Eu-MOF and imidazole

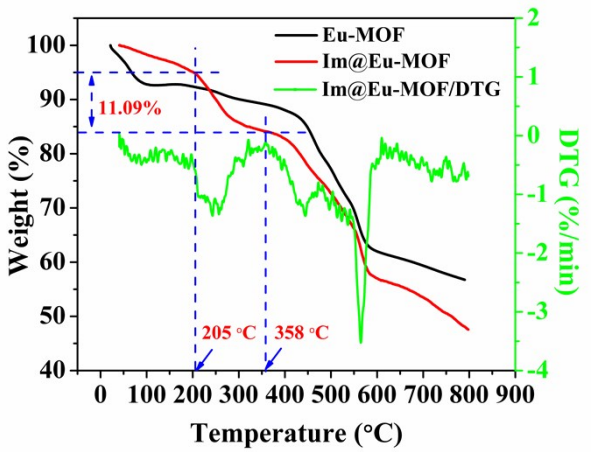


**Figure S4.** The TGA and DTG of Eu-MOF and Im@Eu-MOF

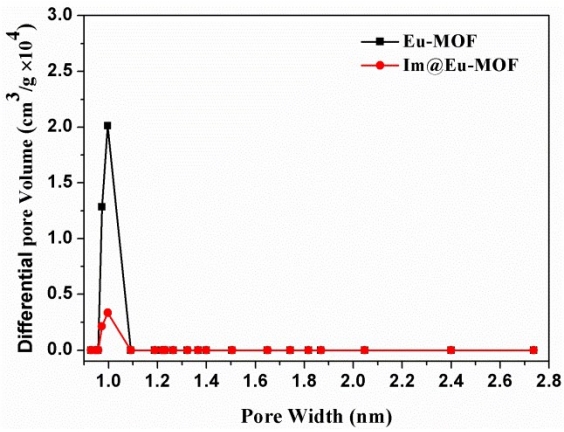


**Figure S5.** pore size distribution profiles for Eu-MOF and Im@Eu-MOF

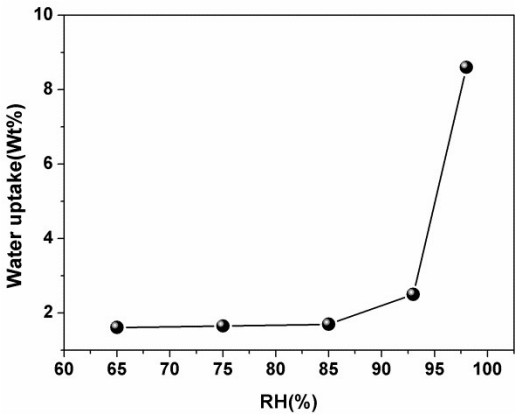


**Figure S6.**Water uptake capacities of Im@Eu-MOF.

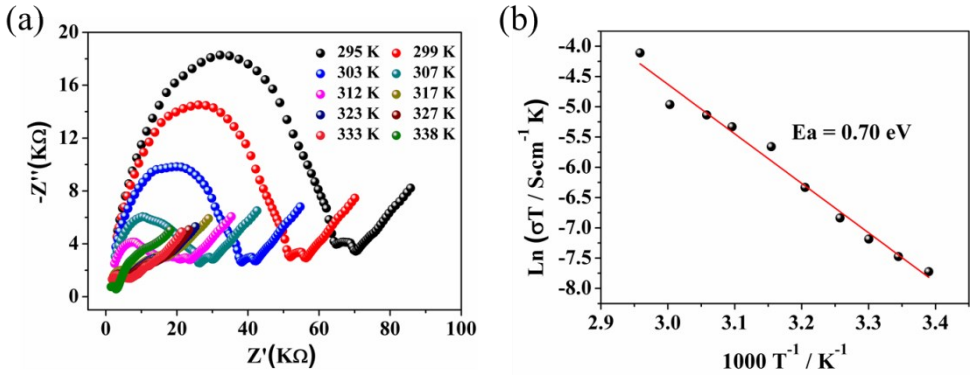


**Figure S7.** (a) Nyquist plats of Eu-MOF at different temperature and 98% RH; (b) Arrhenius plot of Ln(σT) against 1000/T of Eu-MOF under 98% RH (the black solid line represents the best fit of data).

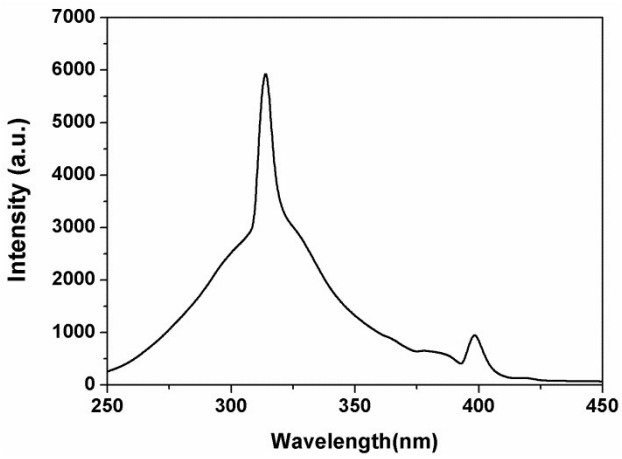


**Figure S8.** Excitation spectrum of Eu-MOF


**Figure S9**. Image of Eu-MOF suspension in water after the addition of various analytes under irradiation of 254 nm UV light

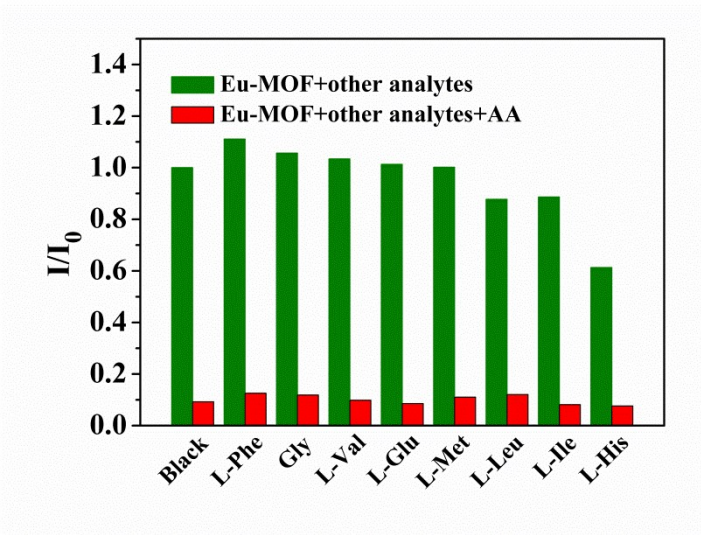


**Figure S10.** Fluorescence intensity ratio histograms of Eu-MOF with the dropping of different analytes (green) and subsequent dropping of AA with the concentration of $10^{-2}$ mol $L^{-1}$ (red) .

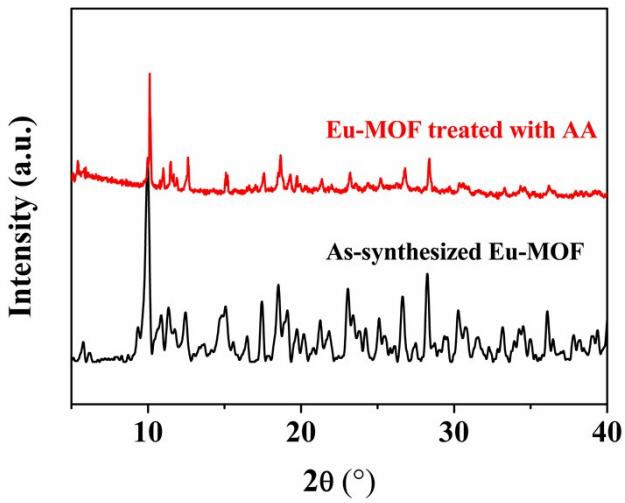


**Figure S11. The PXRD of Eu-MOF after soaking in AA aqueous solution**

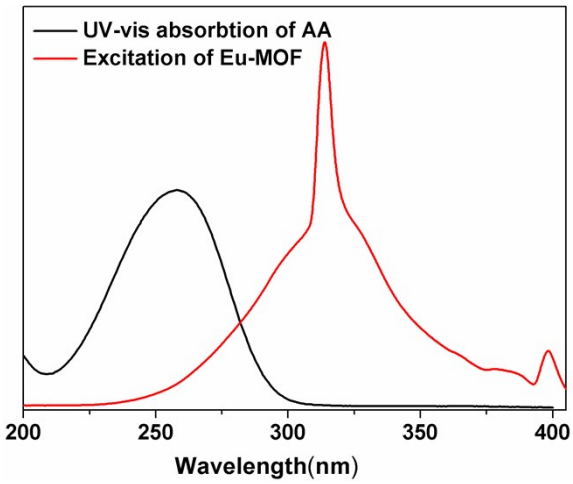


**Figure S12. The excitation spectra of Eu-MOF and the UV-vis absorbtion spectra of AA.**